Eur. Phys. J. Spec. Top. (2025) 234:4711–4722
https://doi.org/10.1140/epjs/s11734-025-01603-1

THE EUROPEAN PHYSICAL JOURNAL SPECIAL TOPICS

Regular Article

Enhanced obesity classification with wavelet packet decomposition and ANN–PSO: a biomedical signal processing approach

Rukiye Uzun Arslan[1,a], Okan Erkaymaz[2,b], İrem Senyer Yapici[3,c], and Matjaž Perc[4,5,6,7,d]

[1] Department of Electrical and Electronics Engineering, Zonguldak Bulent Ecevit University, 67100 Zonguldak, Turkey
[2] Department of Computer Engineering, Turkish Naval Academy, National Defence University, 34942 Istanbul, Turkey
[3] Department of Computer Engineering, Zonguldak Bulent Ecevit University, 67100 Zonguldak, Turkey
[4] Faculty of Natural Sciences and Mathematics, University of Maribor, Koroška Cesta 160, 2000 Maribor, Slovenia
[5] Community Healthcare Center Dr. Adolf Drolc Maribor, Vošnjakova ulica 2, 2000 Maribor, Slovenia
[6] Complexity Science Hub Vienna, Josefstädterstraße 39, 1080 Vienna, Austria
[7] Department of Physics, Kyung Hee University, 26 Kyungheedae-ro, Dongdaemun-gu, Seoul 02447, Republic of Korea

Received 18 February 2025 / Accepted 28 March 2025 / Published online 16 April 2025

Abstract Obesity diagnosis using biomedical signals has received increasing attention in recent years and requires advanced signal processing techniques in order to accurately classify obesity. In this context, this study proposes an intelligent diagnostic system for obesity classification using flash electroretinogram (fERG) signals, with a specific focus on cone responses. A novel feature extraction method based on Wavelet Packet Decomposition (WPD) is employed to decompose the cone responses into high- and low-frequency components, enabling detailed time–frequency analysis with high resolution. Subsequently, statistical features, such as mean, standard deviation, skewness, and kurtosis, are extracted from the decomposed signals and refined to enhance the training of artificial neural networks (ANNs). To optimize model performance, Particle Swarm Optimization (PSO) is integrated with ANN, resulting in an ANN–PSO hybrid model. The experimental dataset, comprising fERG signals from 47 subjects across diverse obesity categories, was utilized to evaluate the proposed hybrid model. The ANN–PSO model demonstrated high classification performance, achieving average accuracies of 95.74% and 96.60% for right and left eye signals, respectively, outperforming traditional ANN models. These findings highlight the effectiveness of WPD in capturing intricate signal characteristics relevant to obesity levels and confirm the potential of the ANN–PSO model as a robust, efficient, and reliable diagnostic tool for clinical applications beyond conventional BMI assessments.

1 Introduction

Obesity is a growing health problem associated with many health problems, such as diabetes, hypertension, musculoskeletal problems, coronary artery disease and premature mortality [1]. It is defined as a chronic disease that occurs as a result of excess fat mass in the body by the World Health Organization (WHO). To classify obesity, it is commonly utilized body mass index (BMI) calculated by dividing body weight in kilogram by the square of the height in meters (kg/m^2). In this context, the most commonly used weight categories based on BMI are as follows: normal weight (BMI 18 to < 25), overweight (BMI 25 to < 30), obese (BMI 30 to < 40), morbid obese (BMI 40 to < 50) and super obese (BMI$\geq$50) [2, 3].

Rukiye Uzun Arslan, Okan Erkaymaz, İrem Senyer Yapici, and Matjaž Perc contributed equally to this manuscript.

[a] e-mail: rukiye.uzun@beun.edu.tr
[b] e-mail: okanerkaymaz@yahoo.com (corresponding author)
[c] e-mail: senyerirem@beun.edu.tr
[d] e-mail: matjaz.perc@gmail.com

Similar to obesity, vision impairment is also considered by WHO as a global public health problem [4]. Irreversible vision loss can occur because of underdiagnoses, delayed diagnosis and delays in treatment [5]. For this reason, the early diagnosis of eye diseases and the choice of the treatment methods are great of importance [6]. In this context, ocular electrophysiological tests, which allow the evaluation of all visual pathways from the retinal pigment epithelium to the occipital cortex, are used frequently used in the diagnosis of eye dysfunction in clinical research. Among them, flash Electroretinogram (fERG) is a comprehensive and non-invasive method that measures the mass response of retinal cells to a light stimulus [7–9]. This test has been used for the diagnosis, monitoring and evaluation of therapeutic interventions efficacy of retinal diseases [1, 10].

The relationship between obesity and eye diseases has been discussed in numerous studies and found that various eye diseases, such as cataracts, diabetic retinopathy, eye pressure (glaucoma) and yellow spot disease (macular degeneration), are associated with obesity [11–27]. The effect of obesity on vision of the eye could sometimes be positive, sometimes negative or sometimes ineffective, so it includes some uncertainty. Furthermore, studies have shown that BMI alone may be inadequate on prediction of the cardiometabolic risk accurately [28, 29]. Therefore, clinicians may have difficulties to explain on how obesity affects eye health. In a recent study, Erkaymaz et al. have investigated the impact of obesity level on a and b waves of fERG signals by applying diverse signal processing methods [30]. They have revealed out that continuous wavelet transform is the most proper method in revealing the effects of obesity on eye signals.

On the other hand, automatic diagnosis of diseases has gradually gained importance to provide assistance for clinicians in recent times. The choice of proper treatment of the disease depends both on accurate diagnosis and correct classification of the disease [6]. In this context, we have recently proposed an automatic diagnostic system classifying obesity levels from fERG signals based on discrete wavelet transform. We have found that artificial neural network-based particle swarm optimization (ANN–PSO) model achieves high classification success as compared traditional artificial neural network (ANN). On the other hand, it is known that wavelet packet decomposition (WPD) gives better resolutions in many application because it takes into account both low and high frequencies of a signal. In this context, in the current study, a framework using WPD is utilized to classify an obesity levels from cone responses of fERG signals recorded from right and left eyes. We have just taken into consideration cone response of fERG signals because it has been put forward that cone response gives more information about obesity as compared with the rod and maximal combined responses [30].

The rest of the paper is organized as follows: in Sect. 2, fERG signal data acquisition, pre-processing, feature extraction and proposed model used for obesity classification have been explained in brief. In Sect. 3, the results have been given. In Sect. 4, conclusion and discussion have been introduced.

2 Methodology

In automatic diagnosis of diseases, feature extraction and classification methods are key factors. Feature extraction is a prerequisite, especially, for classifying multidimensional data sets. This section gives a brief information about feature extraction and classification methods used in the proposed system for classification of obesity levels from three different responses of fERG signals. Figure 1 shows the flow chart of the proposed model.

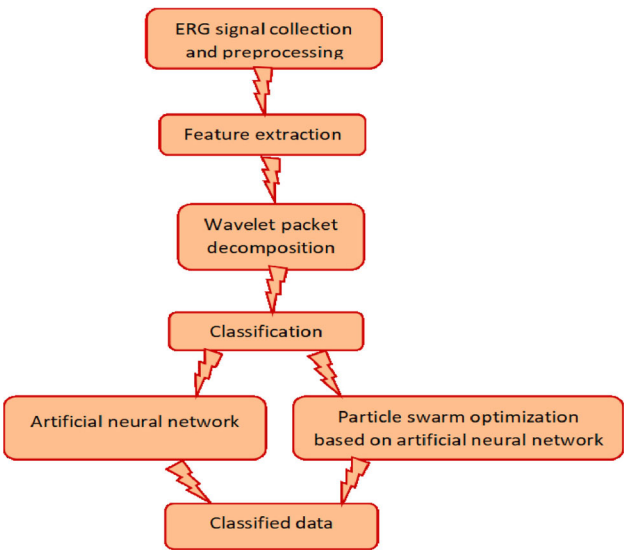

Fig. 1 The flow chart of the proposed model

2.1 fERG signal acquisition

In this experimental study, fERG signals have been acquired from forty-seven volunteers aged between 18 and 70 years with diverse obesity levels namely; normal, overweight, obese, morbid obese and super obese. Volunteers participated in the study have signed a consent form endorsed by the ethics committee of Zonguldak Bülent Ecevit University after all essential explanations are given in detail. Besides, ophthalmological examinations of the volunteers have been examined by a specialist physician.

fERG signals (taken in accordance with ISCEV standards) have been recorded simultaneously from both eyes for flash stimulus at different levels using Metrovision MonPackOne device after (i) dilation of the eyes, (ii) placement of electrodes: Dawson–Trick–Litzkow plus (DTL) type electrodes are placed in the lower conjunctival sac, whereas ground/reference electrodes are attached in the lateral and the middle parts of the forehead, respectively, (iii) 20-min dark adaptation period, and (iv) 15-min light adaptation using the same procedure.

2.2 Preprocessing

In this study, a pre-processing stage is carried out to convert the categorical features in the dataset into numerical values for processing with machine learning methods. At this stage, various transformation and refinement techniques are applied to the dataset in order to improve the performance of the model and ensure that the features are analyzed on a common scale [29]. To this end, the dataset is normalized in the range of 0–1 using the min–max scaling method. Then, feature selection is applied to remove redundant and irrelevant features and improve the performance of the algorithms. Four different feature selection methods are used to identify the features with the strongest association with the prediction of disease recurrence.

Subsequently, the class distribution in the dataset is analyzed to assess the balance between relapsing and non-relapsing patients. The findings show that 28.2% of patients experienced a relapse, while 71.8% did not. This imbalance can introduce a bias toward the majority class, thereby hindering the accurate classification of the minority class. To mitigate this issue, SMOTE, a widely adopted oversampling technique in the training phase, is employed. This approach effectively reduces class imbalance by increasing the representation of the minority class and improves the suitability of the dataset for classification.

2.3 Wavelet packet decomposition

The wavelet transform (WT) operates within a multiresolution analysis framework, providing resolution of a signal in both the time and the frequency domains. However, it has inherent limitations: in the high-frequency domain, it offers high time resolution but low frequency resolution, whereas in the low-frequency domain, it provides high-frequency resolution but low time resolution [31, 32]. WT cannot thus completely capture the particular features of a signal. Higher frequency resolution and timing accuracy of WPD overcome these restrictions, though. This makes WPD a strong pre-processing method for feature extraction since it lets WPD efficiently extract both high- and low-frequency components of a signal. Using a particular mother wavelet, an original signal (S) in WPD is recursively dissected at each level into low-frequency approximation (A) and high-frequency detail (D). Crucially, the decomposition process guarantees that the signal keeps its original information since it neither copies nor reduces already present information [33].

Figure 2 illustrates an example of a 2-level wavelet packet decomposition. As shown, S is divided into D and A components by passing through high-pass (H) and low-pass (G) filters. This procedure divides the signal into several frequency ranges thereby enabling a thorough spectral analysis. Every element follows the same procedure and breaks down even more at the following level. This recurrent breaking down keeps on until a predefined level is attained. At the final stage, four signal components corresponding to different frequency bands are obtained: DD_2, DA_2, AD_2 and AA_2. These components are obtained by passing the signal through two successive high-pass filters (H–H), a high-pass followed by a low-pass filter (H–G), a low-pass followed by a high-pass filter (G–H), and two successive low-pass filters (G–G), respectively.

In addition to its high-frequency resolution and time sensitivity, WPD is also known to give very good results under noisy signal conditions. The shorter and more detailed decomposition of the frequency bands allows noise to be effectively filtered out. This is particularly advantageous in the analysis of biological signals. This capability of WPD provides a significant advantage in biological signal analysis by increasing the reliability of feature extraction in noisy environments [34–36]. In this context, within the scope of this study, the fERG signals are subjected to a 4-level decomposition with the 'db4' wavelet function using the WPD technique. This approach is evaluated as an effective method to remove noise and extract meaningful features from the signal.

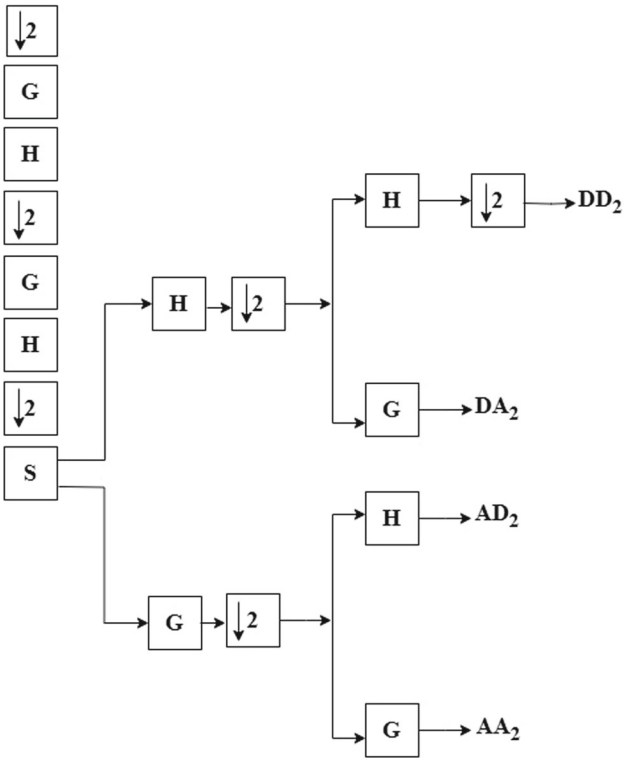

Fig. 2 2-level wavelet packet decomposition diagram

2.4 Feature extraction

Feature extraction is frequently used for object feature data collection and classification. The design and the performance of the classifier considerably depend on both the attribute and characteristic of the selected features. By applying WPD, cone responses of fERG signals are separated into a series of detailed and approximate components which are used as features. Determining the proper features is great of importance for to classify fERG signals. Hence, in this study, various statistical properties, namely mean absolute, standard deviation (STD), average power, skewness, kurtosis, and ratio of the absolute mean values are acquired from the WPD components to find out the main characteristics of the fERG signals.

2.5 Classification-based artificial neural network

Artificial neural networks (ANNs) inspired by the biological human brain have appeared as viable alternatives to conventional techniques. The simple structure of ANN consists of three layers: Input layer, hidden layer and output layer. Each layer possesses a certain number of nodes (or neurons) and interconnections regarding to synaptic weights between neurons in different layers. Diverse ANN architectures, thus various ANN topologies, can be created by connection of neurons as feed-forward or backward. Multilayer perceptron (MLP) is an extensively used ANN topology with input, hidden and output layers whose are fully interconnected via directed feed-forward links [37]. Besides the output of MLP depends on both the weights and the biases, the number of neuron in each layer shows differences [38]. The neuron numbers of input and output layers are determined in accordance with the problem design, whereas the number of hidden layers, the neuron numbers in these layers and the type of activation function are designated using trial-and-error method [39, 40].

In MLP, the initialization of the training process is random, and learning process is ensured by the setting of weights till a certain criteria is obtained. In training process, the reduction of the errors is implemented by applying diverse back-propagation algorithms (such as Quasi-Newton and Levenberg–Marquardt) as backwards from output to input [41]. In the present study, a one hidden layer perceptron feed-forward ANN model is designed with the Levenberg–Marquardt learning algorithm. The neuron number in the hidden layer is ascertained from 8 to 20 neurons by trial-and-error method by implementing 100 trials with a minimum criteria (MSE).

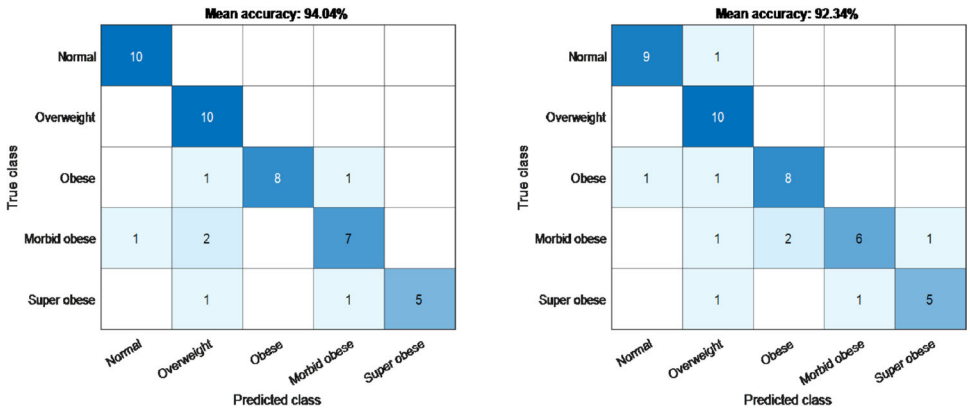

Fig. 3 Cone response for ANN model

(a) The right eye (b) The left eye

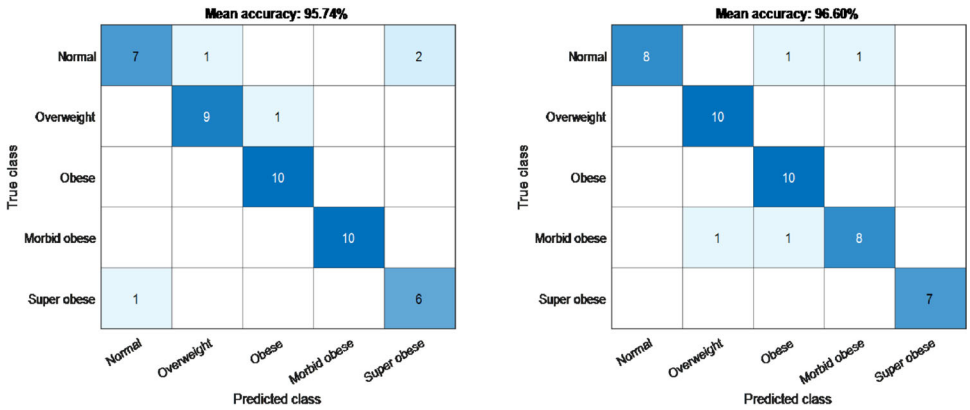

Fig. 4 Cone response for ANN-PSO model

(a) The right eye (b) The left eye

Table 1 Statistical performance of ANN model for cone response of both eyes

			ACC (%)	SEN (%)	SPEC (%)
Right eye	WPD	Normal	97.87	100	97.30
		Overweight	91.49	100	89.19
		Obese	95.74	80	100
		Morbid obese	89.36	70	94.59
		Super obese	95.74	71.43	100
		Average	94.04	84.29	96.22
Left eye	WPD	Normal	95.74	90	97.30
		Overweight	91.49	100	89.19
		Obese	91.49	80	94.59
		Morbid obese	89.36	60	97.30
		Super obese	93.62	71.43	97.50
		Average	92.34	80.29	95.18

Table 2 Statistical performance of ANN-PSO model for cone response of both eyes

			ACC (%)	SEN (%)	SPEC (%)
Right eye	WPD	Normal	91.49	70	97.30
		Overweight	95.74	90	97.30
		Obese	97.87	100	97.30
		Morbid obese	100	100	100
		Super obese	93.62	85.71	95
		Average	94.74	89.14	97.38
Left eye	WPD	Normal	95.74	80	100
		Overweight	97.87	100	97.30
		Obese	95.74	100	94.59
		Morbid obese	89.36	60	97.30
		Super obese	100	100	100
		Average	96.60	92	97.84

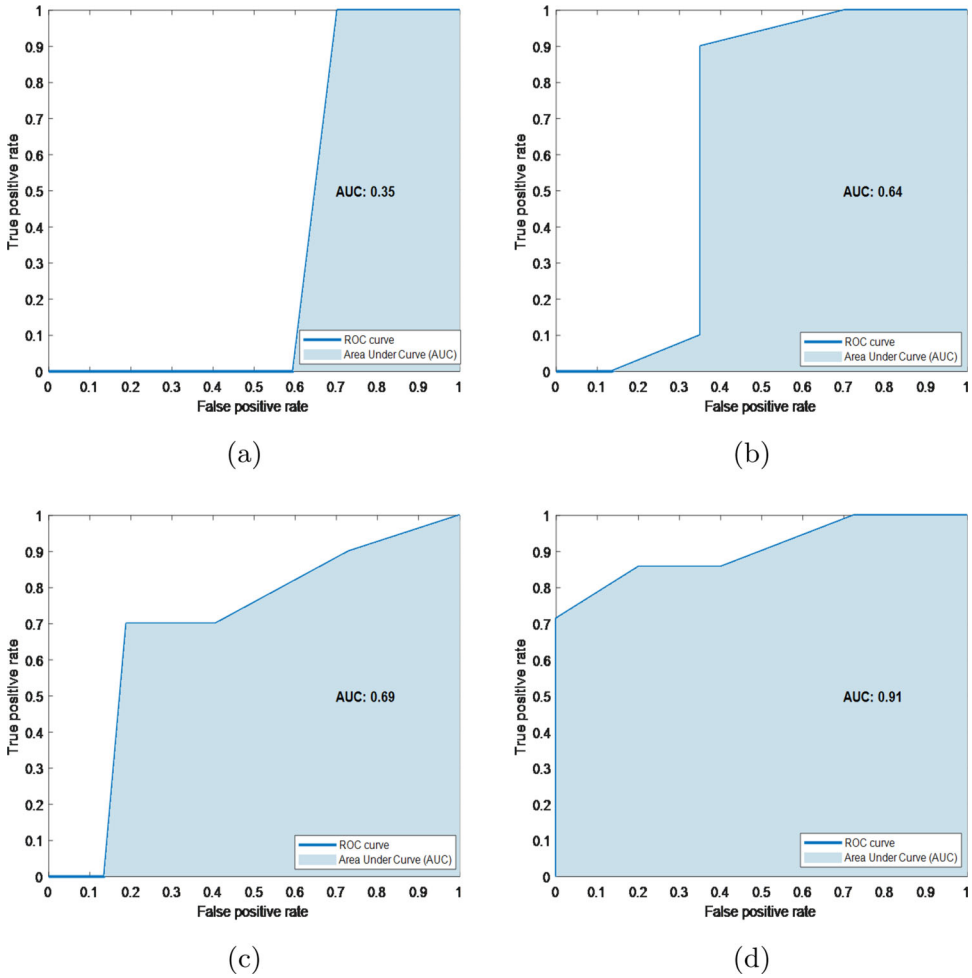

Fig. 5 ROC curves and AUC (area under the ROC curve) values for **a** overweight, **b** obese, **c** morbid obese and **d** super obese level in right eye for ANN model

2.6 Classification ANN-based PSO model

The performance of ANN considerably depends on the network parameters (weights and bias) calculated by learning algorithms. In case of complex nonlinear systems, learning algorithms are quite limited and learning process is also comparatively slow [42]. To discard these drawbacks and obtain the best ANN topology, a particle swarm optimization (PSO)-based ANN model has been proposed where optimization of the network parameters is done by PSO algorithm. The proposed ANN model's topology is 29-H-1, where H shows the hidden neuron number. The training process has been implemented by changing H between 8 and 20 with 100 trials to acquire the optimal neuron number in the hidden layers. Then, PSO algorithm is carried out using these acquired network parameters.

PSO is a stochastic optimization algorithm inspired from social behavior of diverse population of animal species, such as birds, ants, etc. A simplest version of the PSO algorithm operates by owning a population (called a swarm) of feasible solutions (called particles) in the problem space. The operation of the PSO algorithm is defined with the following mathematical expressions:

$$\begin{aligned} V_{i,d}(k+1) =& \mathrm{W}^* V_{i,d}(k) + c_1^* r_1^* (X_{\mathrm{pbest}}(k) - X_{i,d}(k)) \\ &+ c_2^* r_2^* (X_{\mathrm{gbest}}(k) - X_{i,d}(k)) \end{aligned} \tag{1}$$

$$X_{i,d}(k+1) = X_{i,d}(k) + V_{i,d}(k+1) \tag{2}$$

where $V_{i,d}(k)$ and $X_{i,d}(k)$ are velocity and position vectors of ith particle in dimension d at time k, respectively. X_{pbest} is the best position of particle i and X_{gbest} is the global best position of the population [26]. c_1 and c_2 are positive acceleration coefficients set to a positive number as 2. r_1 and r_2 are random numbers having uniform distribution. w and b are the inertia weight and the constraint factor adjusted the velocity's weight, respectively. In the proposed model, each particle is identified by the parameters w and b. The proposed model's flowchart is given in Fig. 1.

2.7 The performance metrics

Model performances are determined using the following metrics:

$$\text{Accuracy (ACC)}(\%) = \frac{\mathrm{TP} + \mathrm{FP}}{\mathrm{TP} + \mathrm{TN} + \mathrm{FP} + \mathrm{FN}} \tag{3}$$

$$\text{Sensitivity (SEN)}(\%) = \frac{\mathrm{TP}}{\mathrm{TP} + \mathrm{FN}} \tag{4}$$

$$\text{Specificity (SPEC)}(\%) = \frac{\mathrm{TN}}{\mathrm{TN} + \mathrm{FP}} \tag{5}$$

Here, ACC is a criterion used to determine the performance of positive samples and gives the overall performance of the model. SEN is the correctly classified ratio of positive samples among all positive samples. SPE is the ratio of exact negative samples among total negative samples. TP (true positive), TN (true negative), FP (false positive) and FN (false negative) represent the number of correctly detected positive samples, the number of correctly detected negative samples, the number of false positives but actually negative and the number of positive samples but falsely detected as negative [6, 43, 44].

3 Results

In this study, the frequency components of cone response in fERG signal are extracted using WPD method due to the fact that it gives better frequency resolution as compared with traditional WT methods. The dimensions of these components (wavelet coefficients) are reduced with six different statistical features (mean, average power, standard deviation, skewness, kurtosis and ratio of the absolute mean value). Thus, a dataset is obtained with 176 features for cone response of 47 subjects including normal, overweight, obese, morbid obese and super obese. We designed an ANN topology with 176 inputs, 1 output and 1 hidden layer (176-H-1) to classify obesity levels. The designed topology is trained with the normalized dataset and 100 trials. Optimum hidden neuron numbers of created topologies for left and right eyes are determined as 6 and 20, respectively. In order to survey the performance of the best topologies, the classification accuracy, the confusion matrix and the receiver operating characteristics (ROC) curves have been used in train–test processes. In the training and testing of ANN models

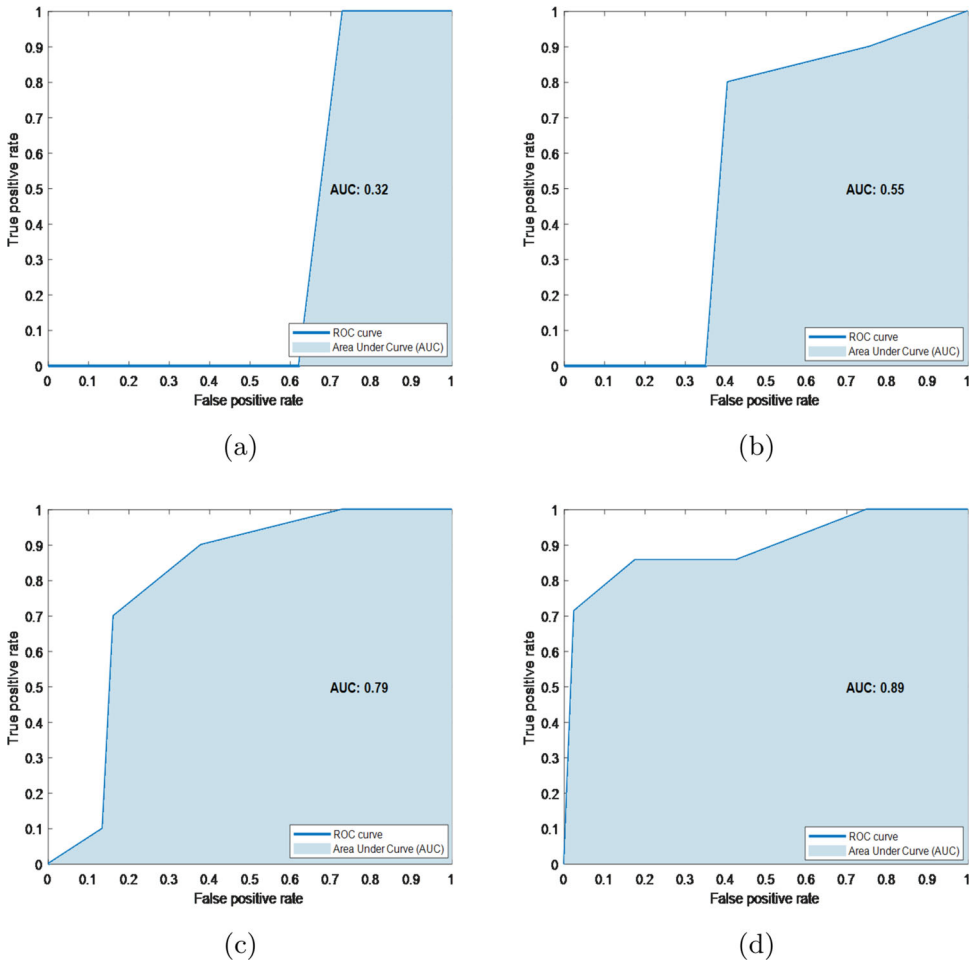

Fig. 6 ROC curves and AUC (area under the ROC curve) values for **a** overweight, **b** obese, **c** morbid obese and **d** super obese level in left eye for ANN model

applied back-propagation learning algorithm, the overall classification accuracy results of the models are given in Figs. 3 and 4.

Average accuracy of ANN-PSO models (right eye = 95.74%, left eye = 96.60%) is better than traditional ANN models (right eye = 94.04%, left eye = 92.34%) in general. The designed model has performed well for the classification of obesity. Then, we also analyze the model performance for each obesity level and test results of the models for left-right eyes are given in Tables 1 and 2.

Table 1 shows the traditional ANN model's performances obtained for the cone responses of both eyes. In the right eye, model performance is high with the rate of 97.87%, 95.74% and 95.74% for normal, obese and super obese subjects, while its performance is below average accuracy (94.04%) with the rate of 89.36% and 91.49% for morbid obese and overweight subjects, respectively. On the other hand, in the left eye, while the model exhibits the best performance for normal (95.74%) and super obese (93.62%) subjects, its performance is below average accuracy (92.34%) for morbid obese (89.36%), obese (91.49%) and overweight (91.49%) subjects.

In Table 2, for right eye, the designed model exhibits the best performance for overweight (95.74%), obese (97.87%) and morbid obese (100%) subjects for the right eye. Its performance is below the average accuracy (95.74%) for normal (91.49%) and super obese (93.62%) subjects. On the other hand, in the left eye, the designed model's performance is 97.87% and 100% for overweight and super obese subjects, whereas its performance is 96.60%, 93.62% and 95.74% for morbid obese, obese and normal subjects, respectively.

In addition, the receiver operating characteristic (ROC) curves and the AUC (area under the ROC curve) values for each obesity levels are achieved and they are demonstrated in Figs. 5, 6, 7 and 8.

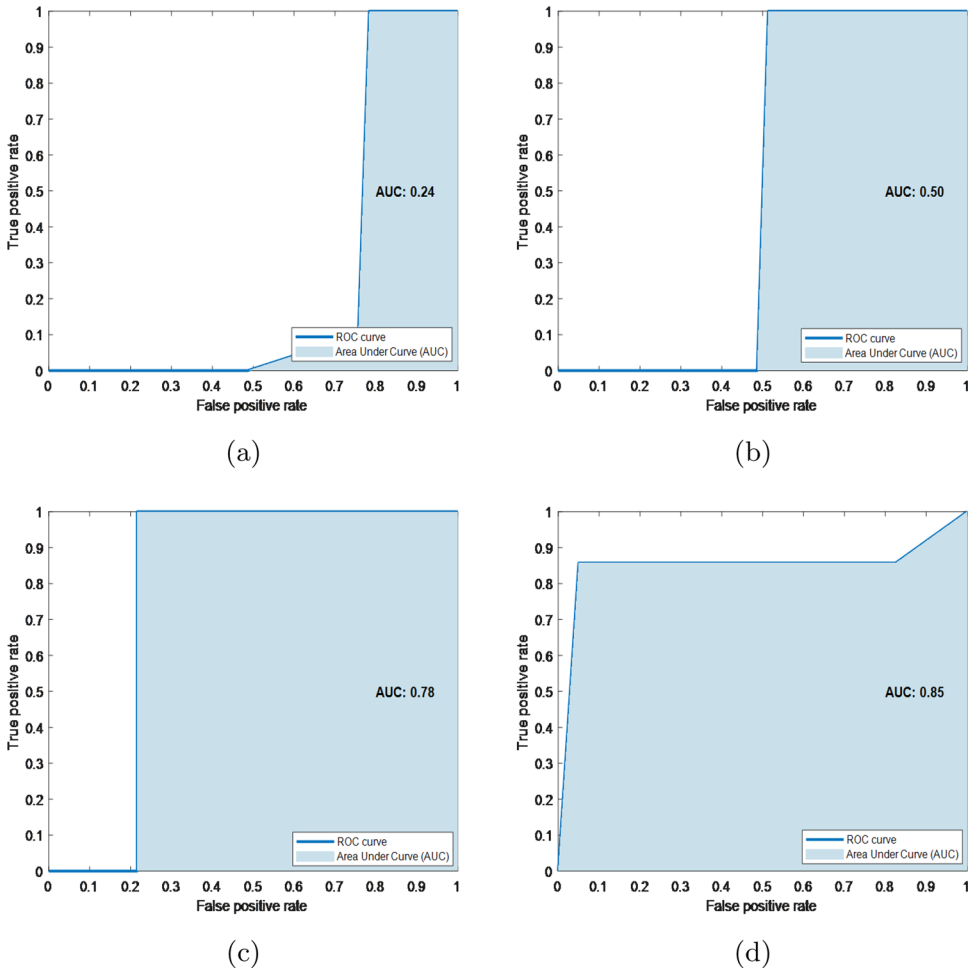

Fig. 7 ROC curves and AUC (area under the ROC curve) values for **a** overweight, **b** obese, **c** morbid obese and **d** super obese level in right eye for ANN–PSO model

4 Discussion and conclusion

Recently, BMI method has not been seen as an adequate criterion for revealing the relationship between obesity and diseases. Therefore, new intelligent decision support models are suggested by scientists to diagnose obesity. In this study different from the literature, efficiency of WPD method to diagnose obesity levels from fERG signals is investigated and a new approach to classify of obesity levels is recommended. To this aim, we use only fERG signal's cone response which has more coded obesity information than the rod and maximal combined responses [30]. The dataset containing six different statistical features of each sub-band obtained by applying WPD on cone responses is created. A traditional ANN and ANN-PSO models are designed by training with this dataset.

Our results indicate that ANN-PSO model exhibits better classification performance than traditional ANN model in determining of obesity levels based on cone responses. In compared model performances, while the proposed model enhances about 1.8% of classifying success for right eye (95.74% of average accuracy), it improves about 4.6% of classifying success for left eye (96.60% of average accuracy), In our previous study in Yapici et al. [29], we designed a hybrid model based on DWT method and showed that the hybrid model performed successfully to classify of obesity levels in cone responses. The model success for right and left eyes is found as 94.04%, 95.74% of average accuracy, respectively. Compared to our previous model [29], the proposed intelligent support system based on WPD has the best classification performance in detecting obesity levels from fERG signals.

The most important advantage of the proposed study is that it uses WPD method based on db4 wavelet, the most suitable feature extraction method for biomedical signals. The WPD method has an effective behavior in suppressing high-frequency noise by applying more and deeper filtering than other frequency analysis methods. On the other hand, the most fundamental limitation of this study is that the performance of the WPD varies depending on the selected wavelet type and the selection of the filtering level. In future studies, we plan to focus on a more detailed investigation of the effect of noise and explore strategies to mitigate its impact to further improve the robustness of the proposed method. These analyses will be contributed to the development of more robust and accurate intelligent decision support systems in the diagnosis of obesity using fERG signals.

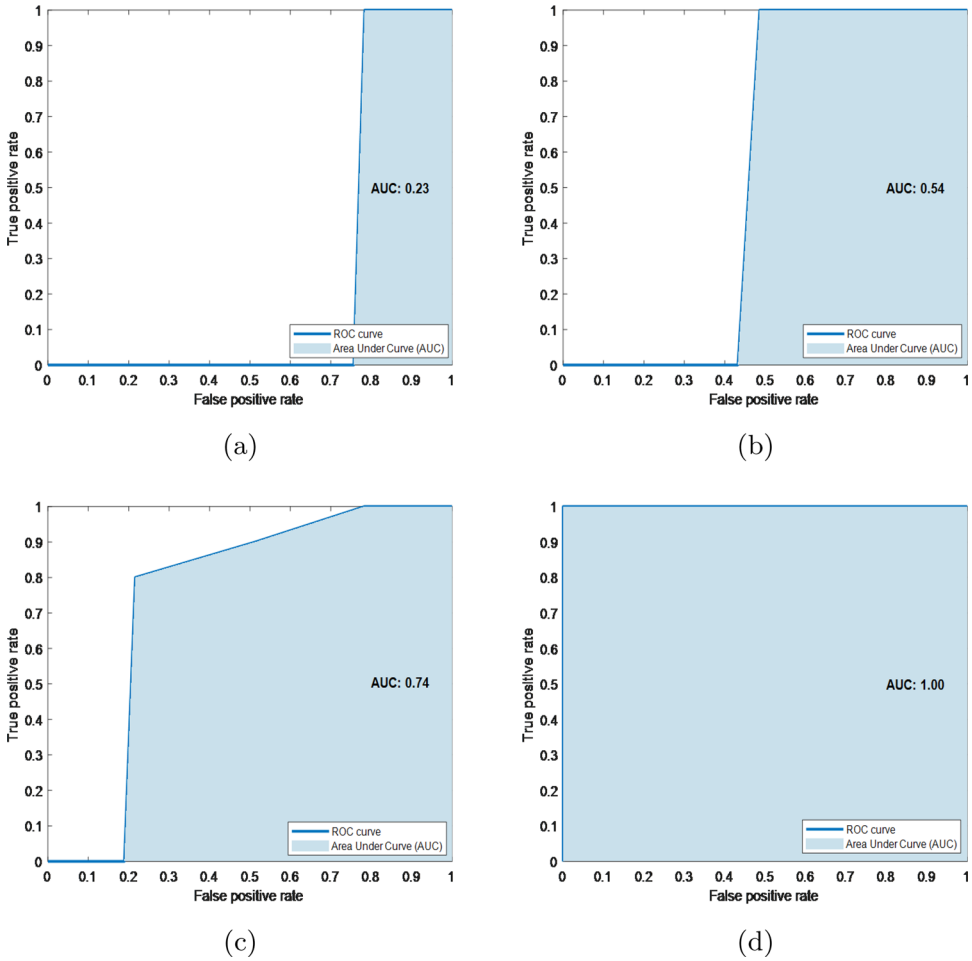

Fig. 8 ROC curves and AUC (area under the ROC curve) values for **a** overweight, **b** obese, **c** morbid obese and **d** super obese level in left eye for ANN–PSO model

Acknowledgements This research is supported by the Scientific Research Project Commission of Zonguldak Bulent Ecevit University under grant number 2017-75737790-01. The study was conducted in accordance with the Declaration of Helsinki, and approved by Clinical Research Ethics Committee of Zonguldak Bulent Ecevit University (Statement of approval number: 2017-66-09/08, 09 August 2017).

Data availability statement The datasets used and analyzed during this study are available from the corresponding author upon reasonable request. However, due to ethical/privacy constraints and institutional policies, we are unable to publicly share the data set. Nevertheless, access to the data can be granted upon reasonable request, provided that the necessary conditions and agreements are met.

References

1. L.J. FrishMan, M.H. Wang, Electroretinogram of human, monkey and mouse. Adler's Physiol. Eye **24**, 480–501 (2011). https://doi.org/10.1016/B978-0-323-05714-1.00024-8
2. B. Doğan, Ö. Can, Obez bireylerde iki farklı yöntemle hesaplanan vücut yağ oranının antropometrik değerler ve lipid parametreleri ile ilişkisi. İstanbul Bilim Üniv. Florence Nightingale Tıp Dergisi **1**(3), 124–128 (2015). https://doi.org/10.5606/fng.btd.2015.023
3. W.H. Organization, *The World Health Report 2000: Health Systems: Improving Performance* (World Health Organization, Geneva, 2000)
4. R.R. Bourne, S.R. Flaxman, T. Braithwaite, M.V. Cicinelli, A. Das, J.B. Jonas, J. Keeffe, J.H. Kempen, J. Leasher, H. Limburg, K. Naidoo, K. Pesudovs, S. Resnikoff, A. Silvester, G.A. Stevens, N. Tahhan, T.Y. Wong, H.R. Taylor, Magnitude, temporal trends, and projections of the global prevalence of blindness and distance and near vision impairment: a systematic review and meta-analysis. Lancet Glob. Health **5**(9), 888–897 (2017). https://doi.org/10.1016/S2214-109X(17)30293-0

5. A.P. Adamis, C.J. Brittain, A. Dandekar, J.J. Hopkins, Building on the success of anti-vascular endothelial growth factor therapy: a vision for the next decade. Eye **34**(11), 1966–1972 (2020). https://doi.org/10.1038/s41433-020-0895-z
6. Y. Kutlu, D. Kuntalp, Feature extraction for ecg heartbeats using higher order statistics of wpd coefficients. Comput. Methods Programs Biomed. **105**(3), 257–267 (2012). https://doi.org/10.1016/j.cmpb.2011.10.002
7. A.Ö. Öner, Oküler klinik elektrofizyoloji. Erciyes Univ Tıp Derg **26**(1), 33–38 (2004)
8. J.R. Heckenlively, G.B. Arden, *Principles and Practice of Clinical Electrophysiology of Vision* (MIT Press, Cambridge, 2006)
9. Latifoğlu, F., Güven, A., Durmuş, U., Öner, A.: Denoising of electroretinogram signals using empirical mode decomposition. In: 2010 15th National Biomedical Engineering Meeting, pp. 1–4 (2010). IEEE
10. Belusic, G.: Electroretinograms. IntechOpen, Rijeka (2011). https://doi.org/10.5772/884
11. Group, A.-R.E.D.S.R., et al.: Risk factors associated with age-related nuclear and cortical cataract: a case-control study in the age-related eye disease study, areds report no. 5. Ophthalmology **108**(8), 1400 (2001). https://doi.org/10.1016/s0161-6420(01)00626-1
12. Group, A.-R.E.D.S.R., et al.: Risk factors associated with age-related macular degeneration: a case-control study in the age-related eye disease study: age-related eye disease study report number 3. Ophthalmology **107**(12), 2224–2232 (2000). https://doi.org/10.1016/S0161-6420(00)00409-7
13. N. Chaturvedi, A.-K. Sjoelie, M. Porta, S.J. Aldington, J.H. Fuller, M. Songini, E.M. Kohner, Markers of insulin resistance are strong risk factors for retinopathy incidence in type 1 diabetes: the eurodiab prospective complications study. Diabetes Care **24**(2), 284–289 (2001). https://doi.org/10.2337/diacare.24.2.284
14. Clemons, T.E., Milton, R.C., Klein, R., Seddon, J.M., Ferris 3rd, F.L.: Risk factors for the incidence of advanced age-related macular degeneration in the age-related eye disease study (areds) areds report no. 19. Ophthalmology **112**(4), 533–539 (2005). https://doi.org/10.1016/j.ophtha.2004.10.047
15. P. Foster, T. Wong, D. Machin, G. Johnson, S. Seah, Risk factors for nuclear, cortical and posterior subcapsular cataracts in the Chinese population of Singapore: the tanjong pagar survey. Br. J. Ophthalmol. **87**(9), 1112–1120 (2003). https://doi.org/10.1136/bjo.87.9.1112
16. M. Henricsson, L. Nyström, G. Blohmé, J. Östman, C. Kullberg, M. Svensson, A. Schölin, H.J. Arnqvist, E. Björk, J. Bolinder, J.W. Eriksson, G. Sundkvist, The incidence of retinopathy 10 years after diagnosis in young adult people with diabetes: results from the nationwide population-based diabetes incidence study in sweden (diss). Diabetes Care **26**(2), 349–354 (2003). https://doi.org/10.2337/diacare.26.2.349
17. R. Hiller, M.J. Podgor, R.D. Sperduto, L. Nowroozi, P.W. Wilson, R.B. D'Agostino, T. Colton, T.F.E.S. Group, A longitudinal study of body mass index and lens opacities: the Framingham studies. Ophthalmology **105**(7), 1244–1250 (1998). https://doi.org/10.1016/S0161-6420(98)97029-4
18. P. Gasser, D. Stümpfig, A. Schötzau, U. Ackermann-Liebrich, J. Flammer, Body mass index in glaucoma. J. Glaucoma **8**(1), 8–11 (1999)
19. B.E. Klein, R. Klein, K.E. Lee, S.C. Jensen, Measures of obesity and age-related eye diseases. Ophthalm. Epidemiol. **8**(4), 251–262 (2001). https://doi.org/10.1076/opep.8.4.251.1612
20. T.-M. Kuang, S.-Y. Tsai, W.-M. Hsu, C.-Y. Cheng, J.-H. Liu, P. Chou, Body mass index and age-related cataract: the Shihpai eye study. Arch. Ophthalmol. **123**(8), 1109–1114 (2005). https://doi.org/10.1001/archopht.123.8.1109
21. D.A. Schaumberg, W.G. Christen, S.E. Hankinson, R.J. Glynn, Body mass index and the incidence of visually significant age-related maculopathy in men. Arch. Ophthalmol. **119**(9), 1259–1264 (2001). https://doi.org/10.1001/archopht.119.9.1259
22. M.C. Leske, A. Connell, S.-Y. Wu, L.G. Hyman, A.P. Schachat, Risk factors for open-angle glaucoma: the Barbados eye study. Arch. Ophthalmol. **113**(7), 918–924 (1995). https://doi.org/10.1001/archopht.1995.01100070092031
23. C. Younan, P. Mitchell, R. Cumming, E. Rochtchina, J. Panchapakesan, K. Tumuluri, Cardiovascular disease, vascular risk factors and the incidence of cataract and cataract surgery: the blue mountains eye study. Ophthalm. Epidemiol. **10**(4), 227–240 (2003). https://doi.org/10.1076/opep.10.4.227.15905
24. J.M. Seddon, J. Cote, N. Davis, B. Rosner, Progression of age-related macular degeneration: association with body mass index, waist circumference, and waist-hip ratio. Arch. Ophthalmol. **121**(6), 785–792 (2003). https://doi.org/10.1001/archopht.121.6.785
25. H.A. Van Leiden, J.M. Dekker, A.C. Moll, G. Nijpels, R.J. Heine, L.M. Bouter, C.D. Stehouwer, B.C. Polak, Blood pressure, lipids, and obesity are associated with retinopathy: the Hoorn study. Diabetes Care **25**(8), 1320–1325 (2002). https://doi.org/10.2337/diacare.25.8.1320
26. N. Cheung, T.Y. Wong, Obesity and eye diseases. Surv. Ophthalmol. **52**(2), 180–195 (2007). https://doi.org/10.1016/j.survophthal.2006.12.003
27. P.F. Jacques, S.M. Moeller, S.E. Hankinson, L.T. Chylack Jr., G. Rogers, W. Tung, J.K. Wolfe, W.C. Willett, A. Taylor, Weight status, abdominal adiposity, diabetes, and early age-related lens opacities. Am. J. Clin. Nutr. **78**(3), 400–405 (2003). https://doi.org/10.1093/ajcn/78.3.400
28. C.N.Y. Ling, S.C. Lim, J.B. Jonas, C. Sabanayagam, Obesity and risk of age-related eye diseases: a systematic review of prospective population-based studies. Int. J. Obes. **45**, 1863–1885 (2021). https://doi.org/10.1038/s41366-021-00829-y
29. İS. Yapici, O. Erkaymaz, R.U. Arslan, A hybrid intelligent classifier to estimate obesity levels based on erg signals. Phys. Lett. A **399**, 127281 (2021). https://doi.org/10.1016/j.physleta.2021.127281

30. O. Erkaymaz, I.S. Yapici, R.U. Arslan, Effects of obesity on time-frequency components of electroretinogram signal using continuous wavelet transform. Biomed. Signal Process. Control **66**, 102398 (2021). https://doi.org/10.1016/j.bspc.2020.102398
31. Chen, Z., Wu, C., Fang, R., Li, Z., Sheng, G., Jiang, X.: Research on leakage current analysis of dc cable based on wavelet packet multi-scale decomposition. In: 2018 Condition Monitoring and Diagnosis (CMD), pp. 1–6 (2018). https://doi.org/10.1109/CMD.2018.8535922 . IEEE
32. Chu, F., Wang, Q., Lu, W.: Detection of the rub location in a rotor system with ae sensors and wavelet analysis. Jixie Gongcheng Xuebao (Chin. J. Mech. Eng.) (China) **38**(3), 139–143 (2002)
33. Gao, R.X., Yan, R.: Wavelet packet transform. In: Wavelets. Springer, Berlin (2011). https://doi.org/10.1007/978-1-4419-1545-0_5
34. S. Mallat, *A Wavelet Tour of Signal Processing*, 2nd edn. (Academic Press, London, 1999)
35. G. Frusque, O. Fink, Robust time series denoising with learnable wavelet packet transform. Adv. Eng. Informat. **62**, 102669 (2024). https://doi.org/10.1016/j.aei.2024.102669
36. P. Xiao, K. Wang, K.H. Ali, Segmentation of heart sound signals using improved Hilbert transform and wavelet packet transform. Circuits Syst. Signal Process. (2025). https://doi.org/10.1007/s00034-025-03000-4
37. M. Bayatvarkeshi, K. Mohammadi, O. Kisi, R. Fasihi, A new wavelet conjunction approach for estimation of relative humidity: wavelet principal component analysis combined with ann. Neural Comput. Appl. **32**(9), 4989–5000 (2020). https://doi.org/10.1007/s00521-018-3916-0
38. S.F. Ardabili, B. Najafi, H. Ghaebi, S. Shamshirband, A. Mostafaeipour, A novel enhanced exergy method in analyzing hvac system using soft computing approaches: a case study on mushroom growing hall. J. Build. Eng. **13**, 309–318 (2017). https://doi.org/10.1016/j.jobe.2017.08.008
39. Ardabili, S., Mosavi, A., Várkonyi-Kóczy, A.R.: Advances in machine learning modeling reviewing hybrid and ensemble methods. In: International Conference on Global Research and Education, pp. 215–227 (2019). Springer
40. S. Sabancı, F. Icier, Effects of vacuum ohmic evaporation on some quality properties of sour cherry juice concentrates. Int. J. Food Eng. **15**(9), 20190055 (2019). https://doi.org/10.1515/ijfe-2019-0055
41. R. Uzun, O. Erkaymaz, I.S. Yapici, Comparison of artificial neural network and regression models to diagnose of knee disorder in different postures using surface electromyography. Gazi Univ. J. Sci. **31**(1), 100–110 (2018)
42. Y. Chakali, A.H. Sadok, M. Tahlaiti, T. Nacer, A pso-ann intelligent hybrid model to predict the compressive strength of limestone fillers roller compacted concrete (rcc) to build dams. KSCE J. Civ. Eng. **25**(8), 3008–3018 (2021)
43. M. Koklu, I.A. Ozkan, Multiclass classification of dry beans using computer vision and machine learning techniques. Comput. Electron. Agric. **174**, 105507 (2020). https://doi.org/10.1016/j.compag.2020.105507
44. Joshi, S., Nigam, B.: Categorizing the document using multi class classification in data mining. In: 2011 International Conference on Computational Intelligence and Communication Networks, pp. 251–255 (2011). https://doi.org/10.1109/CICN.2011.50 . IEEE